

# An enhancement in the photocatalytic activity of TiO<sub>2</sub> by the use of Pd: the question of layer sequence in the resulting hierarchical structure

M. Rezaeian-delouei, M. Ghorbani, M. Mohsenzadeh

© ACA and OCCA 2010

**Abstract** TiO<sub>2</sub> and Pd-modified TiO<sub>2</sub> photocatalysts were prepared by sol-gel method. X-ray diffraction (XRD) data showed that the presence of Pd in TiO<sub>2</sub> catalyst decreases the crystalline size of TiO<sub>2</sub> and stabilizes anatase phase. The study of the photocatalytic activity of the films via Linear Sweep Voltammetry (LSV) plots and antibacterial test against *Escherichia coli* ATCC 25922—a gram negative bacterium—showed that Pd increases the photocatalytic activity of the coatings. Besides, the sequence of layer deposition (TiO<sub>2</sub> and Pd-modified TiO<sub>2</sub>) influences the photocatalytic properties. In other words, more photocatalytic activity is obtained when Pd-modified layer is deposited first.

**Keywords** Titanium dioxide, Sol-gel method, Pd, Photocatalytic activity, Antibacterial test, *E. coli*

## Introduction

Nanosized titanium dioxide as one of the most promising photocatalysts has been widely used in gas and

humidity sensors,<sup>1</sup> self-cleaning and antibacterial coatings,<sup>2–5</sup> and solar cells.<sup>6</sup>

The photocatalytic reaction is initiated by electron-hole pair creation as a result of UV absorption in TiO<sub>2</sub>. Then, the movement of the pair to the surface results in the formation of oxygen and hydroxyl radicals. For photocatalytic microbial inactivation, the reaction between these active radicals and bacteria's cell wall will result in the destruction of cell membrane. More than 20 years ago, photocatalytic microbial inactivation was first reported in references 4, 7, 8. Antibacterial surface provides protection against not only infections and diseases but also odor and allergies.<sup>5</sup>

The photocatalytic activity of TiO<sub>2</sub> is under the influence of its crystalline structure, surface area, crystalline size, bandgap, surface hydroxyl group density as well as the number of electron-hole pairs that participate in the formation of active radicals.<sup>9,10</sup> For most reactions, anatase TiO<sub>2</sub> crystalline structure shows greater photocatalytic activity than rutile one.<sup>11</sup> Smaller crystalline size is usually associated with more photocatalytic efficiency due to increasing the number of photon absorption per unit irradiated area.<sup>3,12</sup> However, smaller crystalline size can also promote the recombination of photogenerated electron-hole pairs when the particle size is below 10 nm.<sup>11</sup>

The deposition of noble or transition metals such as Pt, Au, Ag, Fe<sup>3+</sup>, and Pd on the surface of TiO<sub>2</sub> or doping TiO<sub>2</sub> nanoparticles with these metals can also enhance the photoactivation of TiO<sub>2</sub> catalyst. In this case, an ohmic contact is formed between the metal and the semiconductor and the metal acts as a reduction site.<sup>10,13–16</sup>

TiO<sub>2</sub> coating has been prepared by a number of deposition techniques such as chemical vapor deposition (CVD),<sup>3</sup> sputtering,<sup>17</sup> and sol-gel.<sup>11,12</sup> Sol-gel method is one of the most common methods of producing TiO<sub>2</sub> thin film modified by metal ions. In addition, it offers valuable advantages over other

M. Rezaeian-delouei, M. Ghorbani  
Department of Material Science & Engineering,  
Sharif University of Technology, Azadi Street,  
P.O. Box 11155-9466, Tehran, Iran

M. Ghorbani (✉)  
Institute for Nanoscience and Nanotechnology,  
Sharif University of Technology, Azadi Street,  
P.O. Box 14588-89694, Tehran, Iran  
e-mail: ghorbani@sharif.edu

M. Mohsenzadeh  
Department of Food Hygiene and Aquaculture, Ferdowsi  
University of Mashhad, Azadi Street, P.O. Box 91775-1793,  
Mashhad, Iran

methods due to excellent compositional control, high homogeneity, and feasibility of producing thin films on complex shapes when dip-coating is used.<sup>1,11</sup>

In this study, Pd-modified TiO<sub>2</sub> sols with different amounts of Pd were first prepared. Then, the influence of Pd concentration on crystalline size and crystalline structure of TiO<sub>2</sub> was investigated via X-ray diffraction (XRD) pattern and Transmission Electron Microscopy (TEM) analysis. More importantly, the effect of various loading modes and Pd contents on the separation efficiency of photogenerated carriers was investigated by the use of Linear Sweep Voltammetry (LSV) plots and antibacterial activity of the coating against *E. coli*.

## Materials and methods

### **Preparation of TiO<sub>2</sub> and Pd-modified TiO<sub>2</sub> sols**

The following were used to prepare TiO<sub>2</sub> sol in which the final molar ratio of TTIP:HCl:H<sub>2</sub>O after mixing was 0.1:0.48:530:

- Titanium tetraisopropoxide (TTIP), manufactured by Merck, with a purity of more than 98% as the precursor;
- 37% Hydrochloric acid (HCl), manufactured by Merck as a catalyst for peptization stage; and
- DI water as the dispersing environment.

First, acid–water mixture reached the fixed temperature of 50°C in a reflux system; then, while continuously stirring the mixture, TTIP was added to it. Having added TTIP, the final solution was stirred for 2 h. This method of sol preparation has been previously optimized in an experiment by Mohammadi et al.<sup>1</sup> They reported 0.1 M TiO<sub>2</sub> sol as having the smallest particle size (14 nm).

For the preparation of Pd-modified TiO<sub>2</sub> sols, Palladium acetate (Merck) which had been dissolved in acetic acid by ultrasonic homogenizer (Bandelin 2070) was added to TiO<sub>2</sub> sol and the resulting solution was stirred at room temperature for 2 h in front of a mercury lamp (Philips, 160 W). Therefore, Pd-modified TiO<sub>2</sub> sols containing 0.1, 0.5, 1, and 1.5 wt% Pd were produced.

### **Characterization**

After drying Pd-modified TiO<sub>2</sub> sols, they were calcined in air at 570°C for 1 h. X-ray powder diffraction experiments for these samples were carried out at room temperature with an X-ray diffractometer (Siemens D500) using Cu K $\alpha$  radiation ( $\lambda = 1.5406 \text{ \AA}$ ). The scan ranged from 20° to 80°. Afterward, morphology, crystalline structure, and grain size of

Pd-modified TiO<sub>2</sub> were examined by TEM working at 200 kV (Philips CM-200).

### **Preparation of thin films**

In this study, stainless steel 316 was used as substrate. For preventing the penetration of substrate elements into the coating which can have detrimental influences on the photocatalytic activity, the substrate was coated by a layer of silica.<sup>14</sup> The substrates were sunk into pure TiO<sub>2</sub> sol–gel and Pd-modified TiO<sub>2</sub> sol–gel at 7 mm/min and then pulled out at the same speed after 1 min. The coatings were then dried at 150°C for 15 min. In order to easily refer to the coatings of pure TiO<sub>2</sub> sol–gel and Pd-modified TiO<sub>2</sub> sol–gel, they were labeled T and P, respectively. According to this label-assigning and coating order, three coatings—TT (TiO<sub>2</sub> thin film), TP (with TiO<sub>2</sub> as bottom layer and Pd-modified as surface layer), and PT (with Pd-modified as bottom layer and TiO<sub>2</sub> as surface layer)—were prepared. Finally, all coatings were calcined in air at 570°C for 1 h.

### **Electrochemical experiment**

The LSV plots were investigated in a three-electrode cell, using a potentiostat (273A). The counter electrode was a platinum sheet and saturated calomel electrode (SCE) was used as a reference electrode. The experiments were done at the scanning rate of 5 mV s<sup>-1</sup> and a 1 mol L<sup>-1</sup> KOH aqueous solution was used as the supporting electrolyte. A mercury lamp (Philips, 160 W) was also put in front of the working electrode (the photocatalyst thin film) at a distance of 20 cm.

### **Antibacterial test**

In this study, *E. coli* ATCC 25922 was used as the standard strain. Initially, test strain was inoculated in Brain Heart Infusion Broth (BHI, Merck) and incubated at 37°C for 24 h. After the incubation, one sample of culture was diluted with a saline solution (NaCl 0.9%) up to 0.5 McFarland standard to obtain a bacterial cell density around 10<sup>8</sup> CFU/mL. In the next stage, the dilution process decreased the concentration of the bacteria to 10<sup>6</sup> CFU/mL.

The prepared coatings were sterilized and put in sterile plates. Then, 1 mL of the suspension with the aforementioned concentration was dropped on each specimen. Afterward, the treated plates were incubated at 37°C under a mercury lamp (Philips, 8 W) radiation placed at a 10-cm distance from them. Serial decimal dilutions in the range from 10<sup>-1</sup> to 10<sup>-6</sup> were then prepared from the initial dilution. Bacterial counts were confirmed by plating out of 100 µL of each specimen on Standard Plate Count agar (SPC, Oxoid) after 1, 2, and 4 h after being treated and incubated at 37°C for 24 h.

## Results and discussion

### Characteristics of $\text{TiO}_2$ and Pd-modified $\text{TiO}_2$ photocatalysts

#### XRD analysis

X-ray diffraction patterns of the crystallized  $\text{TiO}_2$  with different amounts of Pd are shown in Fig. 1. All samples exhibit similar patterns; however, the intensity of the peaks changes by increasing Pd content. Peaks marked as “A” and “R” correspond to anatase (JCPDS no. 21-1272) and rutile (JCPDS no. 21-1276) phases, respectively. There is no significant Pd peak in curves; this should be attributed to low ratios of Pd. For samples with anatase and rutile phases, the phase content is calculated by the following equation,<sup>1</sup> where  $X_R$  is the weight fraction of rutile phase in sample and  $I_A$ ,  $I_R$  are X-ray intensity of the anatase (101) and rutile (110) diffraction peaks, respectively:

$$X_R = \frac{1}{1 + 0.79 \left( \frac{I_A}{I_R} \right)} \quad (1)$$

Figure 2 shows the percentage of crystalline phase for each sample. As seen in this figure, the increase of Pd content is followed by an increase in the percentage of anatase phase and a decrease in the formation of rutile crystalline phase. Inhibition of anatase to rutile transformation may be due to an enhancement in phase transformation temperature as a result of surface modification.<sup>13</sup>

Furthermore, increasing Pd content makes the peaks become broader. The presence of broad peaks is ascribed to the small crystalline size. The average anatase crystalline size was estimated using the Scherrer equation<sup>18</sup>:

$$D = \frac{k\lambda}{\beta \cos \theta} \quad (2)$$

In the equation,  $k$  is a constant (0.9)—a shape factor for spherical particle;  $\lambda$  is the X-ray wavelength corresponding to Cu K $\alpha$  radiation;  $\theta$  is the bragg angle (degree); and  $\beta$  is the full width of half-maximum at  $2\theta$  of 25.28°. Table 1 expresses the anatase crystalline size of samples with different Pd contents, according to which the crystalline size of Pd-modified  $\text{TiO}_2$  is lower than that of non-modified  $\text{TiO}_2$ . Increasing Pd content by 1 wt% results in the average crystalline size decreasing by 18%, and the catalyst’s surface area increasing. Zheng et al.<sup>14</sup> reported the same results for Ag presence in  $\text{TiO}_2$  thin films.

#### TEM analysis

The electron diffraction form of Pd-modified  $\text{TiO}_2$  particles with 0.5 wt% Pd is shown in Fig. 3. In this figure, the rings that are marked as “A” and “R” also correspond to anatase and rutile phases of  $\text{TiO}_2$ , respectively. By comparing theoretical d-spacing of each crystal plane for  $\text{TiO}_2$  and Pd and taking into account JCPDS database, one can determine the composition of the nanoparticles. The result reconfirms

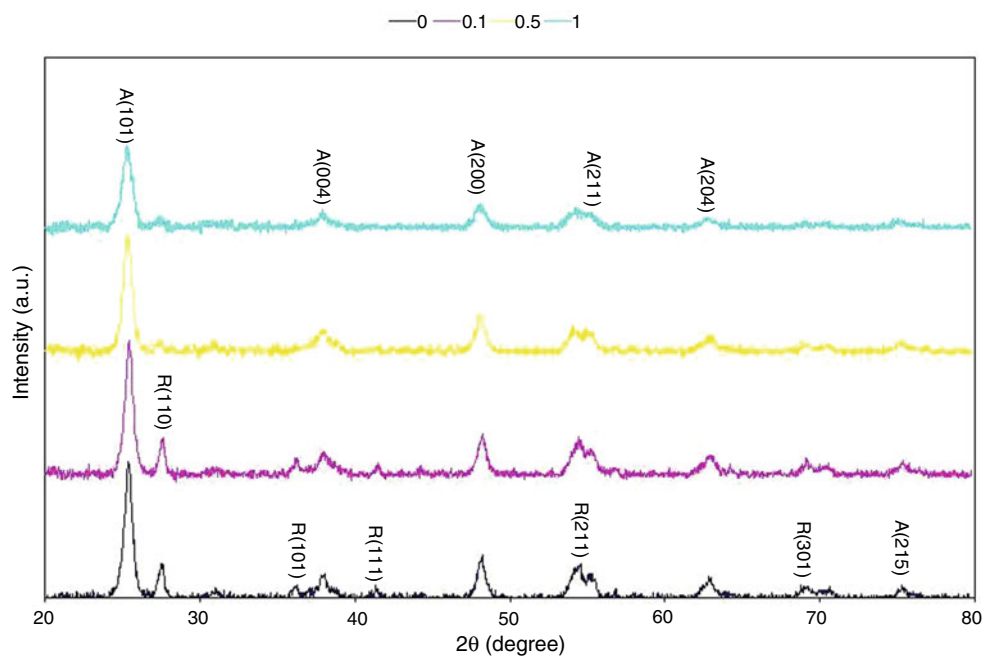


**Fig. 1: X-ray diffraction patterns of the crystallized  $\text{TiO}_2$  with different amounts of Pd**

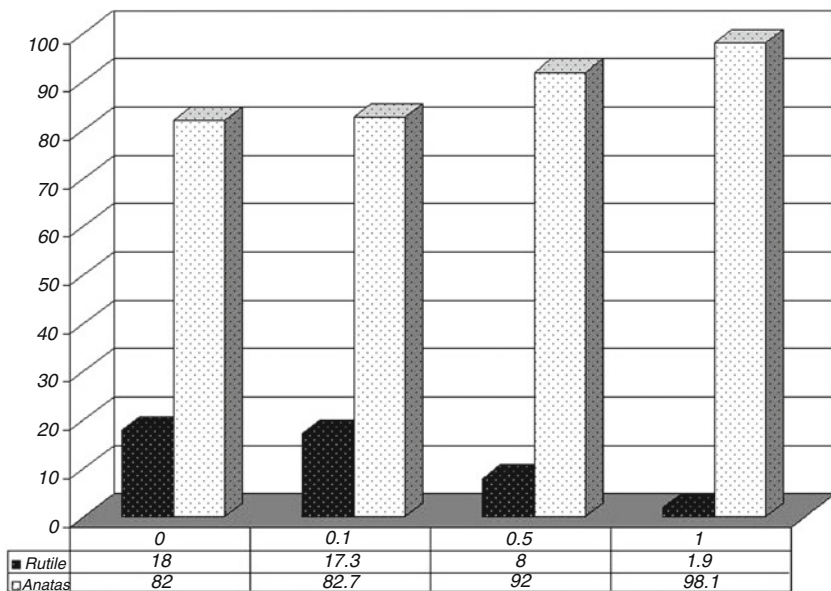


**Fig. 2:** The percentage of crystalline phase (anatase and rutile) for crystallized  $\text{TiO}_2$  with different amounts of Pd

**Table 1:** Anatase crystalline size for samples with different Pd contents

Pd/Ti (wt%)	0	0.1	0.5	1
Anatase crystalline size (nm)	14.5	13.4	12.2	11.9

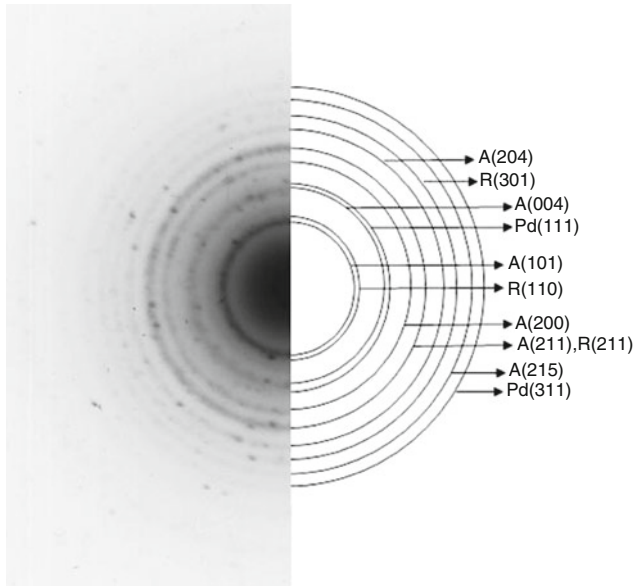


**Fig. 3:** The electron diffraction form of Pd-modified  $\text{TiO}_2$  particles with 0.5 wt% Pd

that  $\text{TiO}_2$  is in anatase phase, although some rings of rutile  $\text{TiO}_2$  are also detected. The presence of metallic Pd which was not confirmed by XRD pattern approved by TEM analysis.

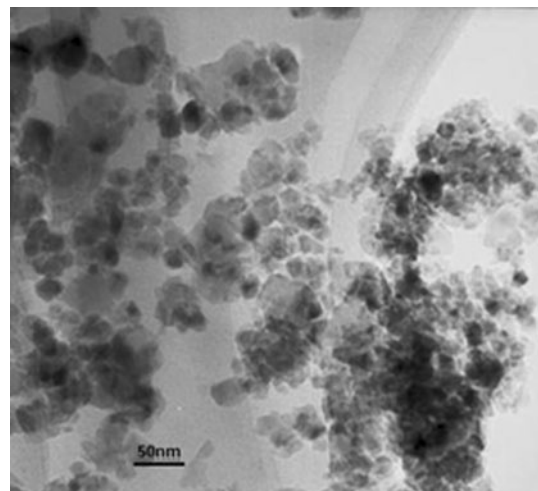


**Fig. 4:** TEM image of Pd-modified  $\text{TiO}_2$  particles with 0.5 wt% Pd

Figure 4 shows the TEM image for this sample. Most of the particles have a size between 10 and 30 nm. Unfortunately, the particles were also found to aggregate during either calcination process or pre-treatment of TEM samples. The TEM image of this catalyst shows that the Pd particles are decorated on  $\text{TiO}_2$  surface.

#### Electrochemical characterization

The LSV plots were investigated to evaluate the photocatalytic activity of the films. Figure 5a shows the LSV plot for TT coating, according to which the maximum current is 17  $\mu\text{A}$ . As KOH solution was used

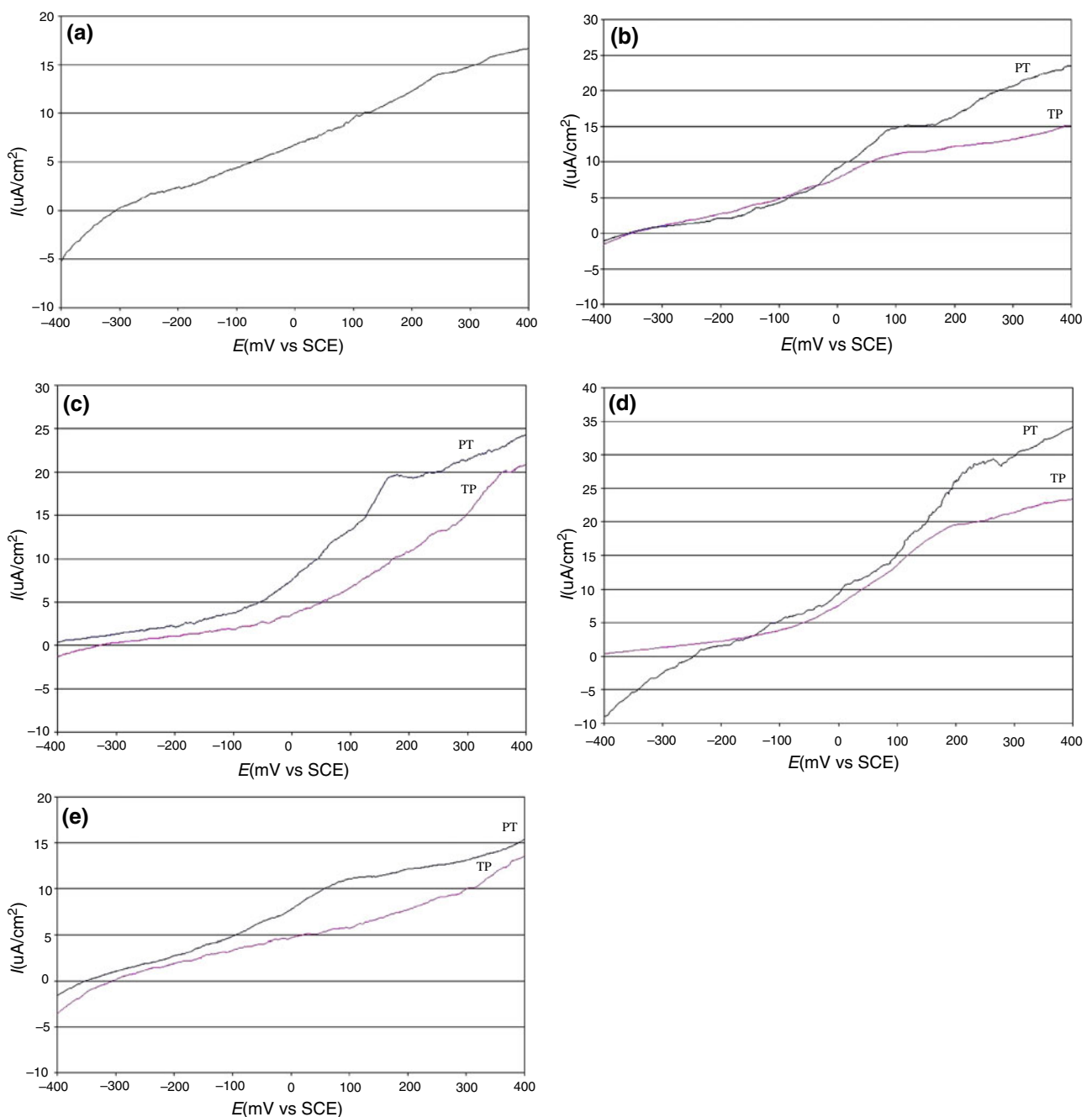
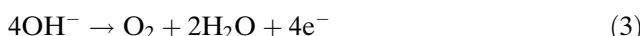


**Fig. 5:** The LSV plots for the prepared coatings with various amounts of Pd under UV illumination in 1 M KOH solution: (a) 0, (b) 0.1, (c) 0.5, (d) 1, and (e) 1.5

as the electrolyte, the following reaction progresses in the solution:



Therefore, the current obtained was roughly the sum total of the current resulting from the above reaction and the photocatalytic current of the coating. Figures 5b–5e demonstrate the LSV plots for PT and TP coatings which contain different amounts of Pd. On

taking a look at the plots, one can easily recognize that the current obtained from PT coatings is more than that of TP ones. The work function of Pd is higher than that of  $\text{TiO}_2$ , which is why when the specimens are put under UV illumination, the electrons migrate from  $\text{TiO}_2$  particles to the surface of Pd particles which results in charge separation and the formation of Schottky barriers at Pd- $\text{TiO}_2$  contact region. The formation of these barriers induces more transmission of electrons from  $\text{TiO}_2$  particles to Pd.<sup>14</sup> As regards PT

films, the presence of Schottky barriers results in the absorption of the electrons in the lower layer and the movement of the holes toward the outer layer of the film. The opposite movement of electron and hole will increase separation efficiency. Besides, PT films have the most efficient UV illumination (the most active  $\text{TiO}_2$  sites) because there is no Pd in the surface to block UV light. However, for TP films, the presence of Schottky barriers will be followed by the movement of the electrons together with the holes to the surface of the specimens. Consequently, the separation efficiency will be less than the time when electron and hole move in opposite directions. Therefore, their photocatalytic activity will be more than TT films but less than PT ones. The presence of the effect of Schottky barriers also shows that Pd is found in the coating in metallic form.<sup>19</sup>

For PT films, the absorption of the electrons in the lower layer accelerates reaction (3) and the system goes into diffusion control condition, as a result of which a peak occurs in these plots. However, for TP plots whose surface layer is Pd-modified  $\text{TiO}_2$ , the interactions between the movement of the electrons to the surface as a result of the existence of Schottky barriers and the transmission of the electrons to the interior of the film as a result of the reaction (3) are determining factors for the absence of any peak in these plots.

Although a comparison between TP and PT plots for each concentration reveals that TP plots show a current decrease, making a comparison among TP plots was indicative of the direct relation between current and Pd content. This shows that although the presence of Pd on the surface layer is an obstacle against UV absorption by  $\text{TiO}_2$  particles, its increase by 1 wt% results in a better charge separation in  $\text{TiO}_2$  particles. A current drop occurs when the amount of Pd goes up to 1.5 wt%. The reason being that although the presence of Pd in  $\text{TiO}_2$  coating increases its photocatalytic efficiency due to the separation of the electron–hole, its presence in excess will have a detrimental effect on  $\text{TiO}_2$  photocatalytic characteristics and make Pd a surface for the electron–hole recombination. On this latter state, the holes will combine with the negative charges collected on the surface of Pd particles and consequently be omitted even before they can participate in the surface reactions. In order to conclude, as the above plots obviously show, 1 wt% Pd is proven to be the optimal concentration in the coating.

### Antibacterial assessments

The results of the antibacterial test were in full agreement with the results obtained from LSV plots. In Fig. 6, the horizontal axis stands for time, and the vertical one stands for the percentage of survived bacteria. According to this figure, UV illumination will eliminate a quarter of the bacteria after 4 h when there

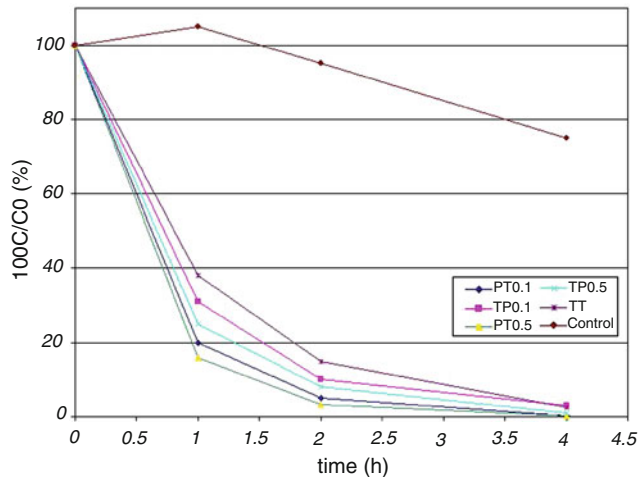


**Fig. 6: Antibacterial test for TT, TP, and PT films with 0.1 and 0.5 wt% Pd: (●) without coating, (\*) TT, (■) TP 0.1, (×) TP 0.5, (◆) PT 0.1, (▲) PT 0.5**

is no coating. However, when the coatings are exposed to UV illumination, an almost complete elimination of the bacteria will occur after 4 h for all coatings. Having made a comparison between the percentages of bacteria destruction for coatings after 2 h, we came to know that the efficiency of bacteria destruction will have the following ascending order: TT, TP 0.1, TP 0.5, PT 0.1, and PT 0.5 (the numbers show the amount of Pd in the coating). Maximum and minimum bacteria elimination will occur for PT 0.5 (more than 96%) and TT (85%), respectively. The same order is true for the current obtained from LSV plots.

In addition, Fig. 6 demonstrates that the highest degree of bacteria destruction happens after the first hour. Therefore, a comparison between bacteria-killing properties of the coatings which contained Pd with those without Pd reveals that the former ones show an increase of 11–35% after an hour.

### Conclusions

According to XRD data, Pd proved to positively influence the photocatalytic properties of  $\text{TiO}_2$  because it decreases the crystalline size of  $\text{TiO}_2$  and stabilizes anatase crystalline phase. The LSV plots indicated that (1) the presence of Pd increases the photocatalytic activity of the coating; (2) PT films have more activity compared with TP ones; and (3) among the values studied, the presence of 1 wt% Pd results in the highest degree of photocatalytic activity. All these three implications were explained by the use of Schottky barriers and active  $\text{TiO}_2$  sites. What is more, the films of  $\text{TiO}_2$  modified by Pd show high antibacterial activity, eliminating the *E. coli* after 2 h UV illumination. The results of this test were in full agreement with the results obtained from LSV plots.

**Acknowledgment** The authors would like to thank Mr. Mohammad Reza Rezaeian-delouei for his kind cooperation in preparing the article.

## References

- Mohammadi, MR, Cordero-Cabrera, MC, Fray, DJ, Ghorbani, M, "Preparation of High Surface Area Titania ( $\text{TiO}_2$ ) Films and Powders Using Particulate Sol-Gel Route Aided by Polymeric Fugitive Agents." *Sens. Actuators B*, **120** 86–95 (2006)
- Parkin, IP, Palgrave, RG, "Self-Cleaning Coatings." *J. Mater. Chem.*, **15** 1689–1695 (2005)
- Evans, P, Sheel, DW, "Photoactive and Antibacterial  $\text{TiO}_2$  Thin Films on Stainless Steel." *Surf. Coat. Technol.*, **201** 9319–9324 (2007)
- Erkan, A, Bakir, U, Karakas, G, "Photocatalytic Microbial Inactivation Over Pd Doped  $\text{SnO}_2$  and  $\text{TiO}_2$  Thin Films." *J. Photochem. Photobiol. A*, **184** 313–321 (2006)
- Daoud, WA, Xin, JH, Zhang, Y, "Surface Functionalization of Cellulose Fibers with Titanium Dioxide Nanoparticles and Their Combined Bactericidal Activities." *Surf. Sci.*, **599** 69–75 (2005)
- Fujishima, A, Rao, TN, Tryk, DA, "Titanium Dioxide Photocatalysis." *J. Photochem. Photobiol. C*, **1** 1–21 (2000)
- Sayılkana, F, Asiltürk, M, Kiraz, N, Burunkaya, E, Arpac, E, Sayılkana, H, "Photocatalytic Antibacterial Performance of  $\text{Sn}^{4+}$ -Doped  $\text{TiO}_2$  Thin Films on Glass Substrate." *J. Hazard. Mater.*, **162** 1309–1316 (2009)
- Skorb, EV, Antonouskaya, LI, Belyasova, NA, Shchukin, DG, Möhwald, H, Sviridov, DV, "Antibacterial Activity of Thin-Film Photocatalysts Based on Metal-Modified  $\text{TiO}_2$  and  $\text{TiO}_2:\text{In}_2\text{O}_3$  Nanocomposite." *Appl. Catal. B*, **84** 94–99 (2008)
- Sakthivel, S, Shankar, MV, Palanichamy, M, Arabindoo, B, Bahneemann, DW, Murugesan, V, "Enhancement of Photocatalytic Activity by Metal Deposition: Characterisation and Photonic Efficiency of Pt, Au and Pd Deposited on  $\text{TiO}_2$  Catalyst." *Water Res.*, **38** 3001–3008 (2004)
- Trapalis, CC, Keivanidis, P, Kordas, G, Zaharescu, M, Crisan, M, Szatvanyi, A, Gartner, M, " $\text{TiO}_2$  ( $\text{Fe}^{3+}$ ) Nanostructured Thin Films with Antibacterial Properties." *Thin Solid Films*, **433** 186–190 (2003)
- Černigoj, U, Lavrenčič Štangar, U, Trešbe, P, Krašovec, UO, Gross, S, "Photocatalytically Active  $\text{TiO}_2$  Thin Films Produced by Surfactant Assisted Sol-Gel Processing." *Thin Solid Films*, **495** 327–332 (2006)
- Liuxue, Zh, Peng, L, Zhixing, S, "Photocatalysis Anatase Thin Film Coated PAN Fibers Prepared at Low Temperature." *Mater. Chem. Phys.*, **98** 111–115 (2006)
- Zhu, B, Li, K, Zhou, J, Wang, S, Zhang, S, Wu, S, Huang, W, "The Preparation of Palladium-Modified  $\text{TiO}_2$  Nanofibers and Their Photocatalytic Performance." *Catal. Commun.*, **9** 2323–2326 (2008)
- Zheng, J, Yu, H, Li, X, Zhang, Sh, "Enhanced Photocatalytic Activity of  $\text{TiO}_2$  Nano-Structured Thin Film with a Silver Hierarchical Configuration." *Appl. Surf. Sci.*, **254** 1630–1635 (2008)
- Araña, J, Garriga i Cabo, C, Doña-Rodríguez, JM, González-Díaz, O, Herrera-Melián, JA, Pérez-Peña, J, "FTIR Study of Formic Acid Interaction with  $\text{TiO}_2$  and  $\text{TiO}_2$  Doped with Pd and Cu in Photocatalytic Processes." *Appl. Surf. Sci.*, **239** 60–71 (2004)
- Crisan, D, Drăgan, N, Crisan, M, Răileanu, M, Brăileanu, A, Anastasescu, M, Ianculescu, A, Mardare, D, Luca, D, Marinescu, V, Moldovan, A, "Crystallization Study of Sol-Gel Un-Doped and Pd-Doped  $\text{TiO}_2$  Materials." *J. Phys. Chem. Solids*, **69** 2548–2554 (2008)
- Kaczmarek, D, Domaradzki, J, Borkowska, A, "Microanalysis of Pd and V-Doped  $\text{TiO}_2$  Thin Films Prepared by Sputtering." *Thin Solid Films*, **515** 6347–6349 (2007)
- Hung, W, Chen, Y, Chu, H, Tseng, T, "Synthesis and Characterization of  $\text{TiO}_2$  and  $\text{Fe}/\text{TiO}_2$  Nanoparticles and Their Performance for Photocatalytic Degradation of 1,2-Dichloroethane." *Appl. Surf. Sci.*, **255** 2205–2213 (2008)
- Wang, W, Zhang, J, Chen, F, He, D, Anpo, M, "Preparation and Photocatalytic Properties of  $\text{Fe}^{3+}$ -Doped Ag@ $\text{TiO}_2$  Core–Shell Nanoparticles." *J. Colloid Interf. Sci.*, **323** 182–186 (2008)